https://doi.org/10.5194/essd-2026-246
Preprint. Discussion started: 12 May 2026

Open Access Earth System Science Data Discussions

A Moderate-Resolution, Long-Term Global Radar-Based Forest Above-Ground Biomass Dataset from 1993 to 2020

Guohua Liu[1,2], Philippe Ciais[3], Shengli Tao[4], Hui Yang[5], Chenwei Xiao[1,2], and Ana Bastos[1,2]

[1]Leipzig University, Institute for Earth System Science and Remote Sensing, 04103 Leipzig, Germany
[2]Max Planck Institute for Biogeochemistry, 07745 Jena, Germany
[3]Laboratoire Sciences du Climat et de l'Environnement, 91191 Paris, France
[4]Institute of Ecology, College of Urban and Environmental Sciences, State Key Laboratory of Vegetation Structure, Function and Construction (VegLab), Peking University, 100871 Beijing, China
[5]College of Urban and Environmental Sciences, Peking University, 100871 Beijing, China

Correspondence: Guohua Liu (guohua.liu@uni-leipzig.de)

Abstract.

Understanding global carbon dynamics and budgets under climate change, land-use shifts, and increasing disturbances remains challenging due to the limitations of existing coarse spatial resolution and short-term or discontinuous biomass datasets. In this study, we generated a new global annual forest above-ground biomass dataset at 8.9 km spatial resolution from 1993 to 2020. This dataset is derived from satellite radar backscatter data and integrates background climate constraints to accounts for regional differences and improve the accuracy of global above-ground biomass mapping. Our dataset estimates an average global forest above-ground biomass carbon stock of 191 $\pm$ 2.5 PgC, aligning with other global estimates. We observed an increase in global forest above-ground biomass carbon stocks from 1993 to 2020 at a rate of 0.29 PgC yr^{-1}. Tropical Africa, temperate and boreal forests are the primary contributors to global forest above-ground biomass carbon stock gains from 1993 to 2020. In contrast, gross above-ground biomass carbon losses are predominantly observed in tropical America and Asia forests, particularly since 2000. This long-term, temporally continuous, and moderate-resolution dataset provides a new benchmark for quantifying biomass carbon dynamics and integrating these processes into Earth System Models. The above-ground forest biomass dataset is openly accessible, alongside this manuscript.

1 Introduction

Terrestrial ecosystem biomass plays a key role in the global carbon cycle (Friedlingstein et al., 2023) and is crucial for developing effective carbon emission mitigation strategies (Bonan, 2008). Above-ground biomass (AGB), the most dominant and dynamic component of terrestrial ecosystems, account for approximately 30% of the total terrestrial carbon sink by sequestering and storing carbon in plant tissues (Beer et al., 2010). However, AGB can also contribute to the terrestrial carbon source, particularly in response to extreme events and disturbances such as drought, wildfires, deforestation, forest degradation (e.g., selective logging, fragmentation) and changes in land use (Liu et al., 2011a; Williams et al., 2016; Qin et al., 2021; Fawcett et al., 2023; Dye et al., 2024). The trade-off of these two impacts on AGB in the context of increasing extreme events and

https://doi.org/10.5194/essd-2026-246
Preprint. Discussion started: 12 May 2026

disturbances determines the carbon dynamics and budgets for terrestrial ecosystems (Reichstein et al., 2013; Frank et al., 2015; Pugh et al., 2019). Therefore, long-term mapping and estimating AGB is essential to understand the carbon dynamics and fate of terrestrial ecosystems, reduce uncertainties in global carbon budget estimates, and formulate land-based and nature-based solutions for climate mitigation policies.

Efforts to map and quantify AGB have primarily relied on field inventories (Pan et al., 2011, 2024), dynamic global vegetation models (DGVMs) (Friend et al., 2014; Ahlström et al., 2017; Yang et al., 2020a), and remote sensing techniques (Saatchi et al., 2011; Baccini et al., 2012; Liu et al., 2015; Xu et al., 2021; Yang et al., 2023). Inventories are a direct and precise way for estimating biomass carbon, supporting the quantification of, for example, global forest carbon changes (Pan et al., 2024) and carbon sources/sinks through Agriculture, Forestry and other Land Use in National Greenhouse Gas Inventories (Tubiello et al., 2021; Bastos et al., 2022). However, large-scale biomass change estimates based on inventory data have inherent limitations: measurements are based on small-scale plots with varying density depending on country/region, limited to forest ecosystems only and are typically carried out at 5-10 years intervals, methodological changes in inventories that may cause artifacts in long term changes, and most tropical forests / un-managed forests are not measured. DGVMs can estimate AGB globally at a coarse spatial resolution (e.g., 0.5°, (El-Masri et al., 2013)), but they often show inconsistencies with carbon flux from atmospheric inversions (Tagesson et al., 2020) due to incomplete representation of biogeochemical processes, disturbances and forest management (Pugh et al., 2019). Compared to these two approaches, remote-sensing has emerged as a promising way of quantifying forest biomass carbon in a spatially and temporally continuous manner and with global coverage. Currently, static AGB maps for specific years and dynamic continuous AGB maps have been produced using optical (Gibbs and Ruesch, 2008; Hu et al., 2016; Yang et al., 2020b), lidar (Saatchi et al., 2011; Baccini et al., 2012; Xu et al., 2021), radar (Besnard et al., 2021; Santoro et al., 2021), and passive microwave (Liu et al., 2015; Fan et al., 2019; Yang et al., 2023) techniques. Static AGB maps, generated at high spatial resolutions from 100 to 1000 meters, offer detailed spatial distribution insights and serve as baselines for future carbon stock change estimates. However, they mainly provide a snapshot of biomass at a single year, lacking information on temporal changes. This limitation makes it challenging to identify AGB temporal dynamics, despite AGB's large temporal variability.

Dynamic continuous AGB maps offer opportunities to monitor AGB dynamics. For instance, pantropical or global dynamic continuous AGB maps (Liu et al., 2015; Fan et al., 2019; Besnard et al., 2021; Yang et al., 2023) with a spatial resolution of 25 km were produced using vegetation optical depth (VOD) around 10 years or radar satellite data from 1992-2018. These products have contributed to improve our understanding of biomass carbon dynamics, for example to map carbon losses and gains due to deforestation, forest degradation and management (Heinrich et al., 2021; Xu et al., 2021; Fawcett et al., 2023; Heinrich et al., 2023), quantify biomass responses to disturbances such as droughts or fires (Fan et al., 2023, 2024), evaluate reported sinks/sources by national greenhouse gas inventories (Fang et al., 2024; Lauerwald et al., 2024) and quantify drivers of trends in regional carbon budgets (Winkler et al., 2023). However, most current satellite biomass products either have limited long-term biomass records (for instance European Space Agency's Climate Change Initiative (CCI) data, 2010, 2017-2021 available) (Santoro and Cartus, 2023) or coarse spatial resolution of 25 km (Yang et al., 2023) which can lead to a loss of accuracy in predicting carbon dynamics due to averaging.

https://doi.org/10.5194/essd-2026-246
Preprint. Discussion started: 12 May 2026


Open Access Earth System Science Data Discussions

AGB dynamic changes mainly result from three processes: physiological processes such as photosynthesis and growth, natural disturbances and recovery, and anthropogenic activities like land use changes (Houghton et al., 2009). These processes influence on AGB is usually slow-in and fast-out, and also legacy effects and slow recovery (Harris et al., 2016; Yang et al., 2020c). Large-scale and instantaneous impacts could be detected by the current short-term and coarse AGB dataset. However, evaluating the impacts on biomass carbon from slow-developing and small-scale processes such as biotic disturbances, tree mortality, or recovery dynamics requires high-resolution and long-term biomass data (McDowell et al., 2015). To circumvent these issues, space for time substitution based on high resolution biomass maps such as the ESA-CCI ones is often used to quantify AGB changes due to following disturbances (Xu et al., 2021; Yang et al., 2023; Feng et al., 2024). However, space for time substitution relies on the assumption that other environmental factors contributing to spatiotemporal variability in biomass can be ignored, which might not hold under the current pace and magnitude of global environmental change.

The recent long-term radar backscatter data by Tao et al. (2023) provides a valuable opportunity to map biomass changes globally at moderate spatial resolution (8.9 km) and over almost three decades. Based on this new dataset, we generate a new long-term and moderate-resolution global AGB dataset from 1993 to 2020 through a machine learning upscaling model trained on AGB data from ESA CCI and including additional climatic predictors. We then quantify global and regional above-ground biomass carbon stocks, and their spatial and temporal variability over the study period.

2 Materials and Methods

2.1 Data

2.1.1 Land cover data

The annual ESA-CCI global Plant Functional Types (PFT) dataset (v2.0.82) at 300 m spatial resolution from 1993 to 2020 (Harper et al., 2023) was used in this study. This dataset provides the percentage cover of 14 PFTs. We define forest following the Food and Agriculture Organization (FAO) definition, where tree cover >= 10%, excluding land predominantly under agricultural or urban use. Tree cover in this PFT dataset includes Broadleaved Evergreen (BE), Broadleaved Deciduous (BD), Needleleaved Evergreen (NE), and Needleleaved Deciduous (ND) trees. We calculated the total tree cover percentage at the 8.9 km resolution and excluded pixels where urban and agricultural land cover exceeded 50%. This resulted in a global forest study area at 8.9 km resolution.

To define biome-level patterns, we integrated the FAO global ecological zones (https://data.apps.fao.org/catalog/dataset/2fb209d0-fd34-4e5e-a3d8-a13c241eb61b, Table S1) with the ESA-CCI forest maps (Harper et al., 2023). Based on this integration, we classified global forests into seven major biome groups: tropical American forest, tropical African forest, tropical Asian forest, subtropical forest, temperate forest, and boreal forest (Figure S1).

https://doi.org/10.5194/essd-2026-246
Preprint. Discussion started: 12 May 2026

2.1.2 Biomass reference data

Here we used the global above-ground biomass (Mg ha^{-1}) maps at 100 m spatial resolution for the years 2017-2020 from the European Space Agency's Climate Change Initiative version 6 (Santoro and Cartus, 2025) as reference data. To match the spatial resolution of the radar backscatter data, the 100 m ESA-CCI biomass maps were aggregated to 8.9 km using spatial averaging. As this dataset was developed for forest above-ground biomass, we extracted forest AGB based on ESA-CCI forest maps. Additionally, low-quality ESA-CCI AGB data were filtered based on the standard deviation, excluding pixels where the coefficient of variation exceeded 80%.

2.1.3 Inventory biomass data

We compiled forest inventory above-ground biomass data from previous studies that is publicly available (Anderson-Teixeira et al., 2018; Brienen et al., 2015; Qie et al., 2017; Schepaschenko et al., 2019). The inventory data were collected over the period 1993–2020 at the plot scale. For each study, we extracted the above-ground biomass variable as follows: 'biomass_ag_OM' from Anderson-Teixeira et al. (2018), 'AGB_ini' and 'AGB_fin' from Brienen et al. (2015), and 'Initial AGB' from Qie et al. (2017) and Schepaschenko et al. (2019), all with units in Mg ha^{-1}. The inventory plots were aggregated to our 8.9 km grid cells, and only grid cells containing more than 10 inventory plots were retained to ensure sufficient sampling density (Figure S2). For each selected grid cell, we calculated the mean AGB by averaging all inventory plot values within that grid cell.

2.1.4 Satellite radar backscatter data

To estimate long-term AGB, we used the temporally-continuous radar backscatter dataset from satellite developed by Tao et al. (2023). The dataset merged signals from the C-band European Remote Sensing satellite (ESA, 1992-2001)/ Advanced SCATterometer (ASCAT, 2007-2020) and Ku-band Quick Scatterometer (QSCAT, 1999-2009). The resulting dataset provides long-term monthly satellite radar backscatter from 1992 to 2020, covering most global land areas at a resolution of approximately 8.9 km, therefore higher than the commonly used 25 km resolution in other global AGB reconstructions (e.g., Liu et al. (2015); Besnard et al. (2021); Yang et al. (2023)).

Radar backscatter is considered a useful indicator for AGB, but it is also influenced by variations in vegetation water content (VWC) and surface water (Liu et al., 2011b; Konings et al., 2019; Wigneron et al., 2021). Separating the biomass signal from the vegetation water content is challenging with the current data available, so that careful pre-processing is needed in order to minimize the effect of variations in VWC in radar-derived AGB estimates. It is generally agreed upon, that the longer the time scales, the smaller the effect of VWC vs. biomass changes (Konings et al., 2019). Therefore, previous studies using radar data to infer changes in AGB have used temporal smoothing approaches (Yang et al., 2023), or used annual values (Fan et al., 2019; Qin et al., 2021; Li et al., 2025) aggregated for the wet-season (often taken as the annual maximum values), so that interannual variations better match changes in AGB, and not VWC.

In our study, we first evaluated different pre-processing approaches in order to derive annual radar backscatter values that minimize VWC-related effects the most: the yearly mean and maximum values of radar backscatter, the mean radar backscatter

https://doi.org/10.5194/essd-2026-246
Preprint. Discussion started: 12 May 2026

during a regionally fixed wet season, and the mean radar backscatter during a locally defined wet season. For yearly mean and maximum estimates, we first smoothed the data to remove short-term noise, by applying the 3-, 6-, and 12-month moving averages to the original monthly radar backscatter time series.

The regionally fixed wet season calculation followed the approach used in Yang et al. (2023), defined as May–August in the Northern Hemisphere and November–February in the Southern Hemisphere. The locally defined wet season was determined using monthly soil moisture (SM) from ESA CCI SM v07.1 and ERA5-Land SWVL1 for 1993–2020. Soil moisture data were interpolated to the radar grid (8.9 km) using bilinear interpolation. To avoid biases from long-term trends, soil moisture time series at each grid cell were linearly detrended prior to analysis. Wet season were identified using a percentile-based threshold: months with detrended soil moisture exceeding the 66thth percentile of the local distribution were classified as wet months. The mean radar backscatter during the locally defined wet season was then calculated using both the original monthly and a 3-month moving averaged radar time series.

We quantified the correlation between each radar backscatter index (derived from different approaches) and soil moisture to identify the radar backscatter index least influenced by hydrological variability. Among all indices tested, the locally defined wet-season mean radar backscatter derived from the original monthly time series exhibited the lowest correlation with soil moisture (Figure S3). This result suggests that this approach minimizes the confounding effects of drought stress and VWC variability compared to the other indices evaluated. Therefore, we selected the time series of radar backscatter averaged over the locally defined wet season for all subsequent analyses.

To further reduce potential errors, we excluded pixels identified as outliers based on standard deviation thresholds (beyond a threshold of four standard deviations). Because this study focuses on AGB over forests, forest radar backscatter data were obtained using ESA-CCI forest maps (Harper et al., 2023). Moreover, pixels with more than 80% coverage of regularly flooded wetlands or lakes were removed using the global wetland dataset from Tootchi et al. (2019). We also excluded pixels with peatland fractional coverage greater than 10% based on the global peatland map from Melton et al. (2022). Finally, we excluded data from 1992 due to substantial spatial gaps in radar observations during that year.

2.1.5 Climatic variables

We use monthly maximum temperature, minimum temperature and total precipitation from the TerraClimate (https://www.climatologylab.org/terraclimate.html) dataset, which has a spatial resolution of ~4 km and covers the period from 1991 to 2020 (Abatzoglou et al., 2018).

Given that TerraClimate only provides monthly maximum and minimum temperatures, we averaged these two variables to derive monthly mean temperature. To characterize background climate conditions, we computed mean annual temperature (MAT_bg) and mean annual precipitation (MAP_bg) over the period 1991–2020. These variables represent long-term climatic means that constrain regional biomass potential. To account for interannual climate variability from 1993 to 2020, we also calculated yearly mean temperature (MAT_dyn) and yearly total precipitation (MAP_dyn) for each year. These dynamic climate variables were used to test whether short-term climate variability improves AGB prediction beyond background climatic controls. To ensure consistency with the radar backscatter dataset, these variables were aggregated to 8.9 km resolution us-

https://doi.org/10.5194/essd-2026-246
Preprint. Discussion started: 12 May 2026

ing Climate Data Operators (CDO) remapping: bilinear interpolation (remapbil) for temperature and conservative remapping (remapcon) for precipitation.

2.2 Methods

2.2.1 Machine learning model

We trained global random forest regression models to estimate AGB using radar backscatter (Rad) as the primary predictor and ESA-CCI AGB maps (2017–2020) as the training target. Because the relationship between radar backscatter and AGB may vary across climatic regions, we tested models incorporating background climate variables (MAT_bg and MAP_bg). To further evaluate whether interannual climate variability improves model performance, we also tested models including dynamic climate variables (MAT_dyn and MAP_dyn). In total, three global random forest models were evaluated based on combinations of radar backscatter and climate predictors (Table 1).

To ensure robust evaluation, we implemented a spatiotemporal block cross-validation framework. Specifically, the year 2020 was reserved as an independent test set. Data from 2017–2019 were partitioned into spatial–temporal blocks, with 80% used for training and 20% for validation in each iteration. This design reduces spatial and temporal autocorrelation biases and enhances model generalization.

Model performance was evaluated using root mean square error (RMSE), coefficient of determination (R^2), and Bayesian information criterion (BIC) for training, validation, and testing datasets. Performance metrics were averaged across cross-validation iterations. The optimal model was selected based on the lowest BIC value, balancing predictive accuracy and model complexity.

Model uncertainty (Unc) was quantified as the variability among predictions generated across cross-validation iterations, calculated according to Equation 1.

$$\mathrm{Unc} = \mathrm{std}_{k=1}^{K}\left(\frac{1}{n_k}\sum_{j=1}^{n_k}\left(\mathrm{obs}_{kj} - \mathrm{pred}_{kj}\right)\right) \tag{1}$$

where Unc is the model uncertainty, K is the total number of cross-validation iterations (models), n_k is the number of observations in iteration k, obs_{kj} and pred_{kj} are the observed and predicted AGB values for observation j in cross-validation iteration k, and $\mathrm{std}_{k=1}^{K}$ denotes the standard deviation computed across all K iterations of the mean prediction errors.

2.2.2 Analysis of spatial and temporal dynamics

We further applied the best-performing random forest model to predict global AGB over the study period from 1993 to 2020 using satellite radar backscatter data. Above-ground biomass carbon (AGC) was estimated by multiplying the AGB by a factor of 0.49 (Equation 2).

$$\mathrm{AGC} = \mathrm{AGB} \times 0.49 \tag{2}$$

https://doi.org/10.5194/essd-2026-246
Preprint. Discussion started: 12 May 2026

where, AGC is the above-ground biomass carbon, AGB is the above-ground biomass, 0.49 represents the average carbon fraction in dry biomass (Saatchi et al., 2011).

Below-ground biomass carbon (BGC) was estimated using the global root-to-shoot ratio map developed by Huang et al. (2021). Total ground live biomass carbon (TGC) was calculated as the sum of AGC and BGC. The coefficient of variation (CV) is calculated as the ratio of the standard deviation (σ) to the mean (μ), expressed as a percentage:

$$\mathrm{CV} = \left(\frac{\sigma}{\mu}\right) \times 100 \tag{3}$$

where σ is standard deviation of AGC density, μ is mean AGC density.

AGC stock for each pixel was derived by multiplying AGC density by the pixel area. To evaluate changes of carbon storage in above-ground biomass over time, we computed the net AGC stock change for each biome by analyzing the differences in AGC stock between two time points (Equation 4). Given the slow rate of net AGC stock change, we calculated the mean decadal AGC change for three distinct periods: 1993–1999, 2000–2009, and 2010–2019.

$$\mathrm{AGC}_{\mathrm{net}}(t) = \mathrm{AGC}(t) - \mathrm{AGC}(t-1) \tag{4}$$

where $\mathrm{AGC}_{\mathrm{net}}(t)$ represents the net AGC stock change for the year t, and $\mathrm{AGC}(t)$ and $\mathrm{AGC}(t-1)$ are the AGC stocks at year t and $t-1$, respectively.

3 Results

3.1 Above-ground biomass model performance

The performance of the three AGB models varies significantly based on the predictors used and their ability to generalize to unseen spatial area and unseen year (Table 1). The random forest regression model based solely on radar backscatter (Rad model) achieved a high coefficient of determination (R^2 = 0.884) in the training dataset but performed poorly in validation (R^2 = 0.175) and testing (R^2 = 0.136), indicating severe overfitting and poor generalization. This lack of generalization was further reflected in high RMSE values for the validation (83.3 Mg ha^{-1}) and testing (85.2 Mg ha^{-1}) datasets.

Incorporating background climate variables substantially improved model performance. The Rad-Clim_bg model increases R^2 to 0.977 (training), 0.815 (validation), and 0.833 (testing), while markedly reducing RMSE and BIC across all datasets. Compared with the Rad model, RMSE decreased by 43.9 Mg ha^{-1} and 47.7 Mg ha^{-1} in the validation and testing datasets, respectively. BIC decreased by approximately 17–18%. These results demonstrate that background climate variables provide critical information for accurate AGB estimation and greatly enhance model generalization.

To assess whether dynamic climate variables provide additional predictive power beyond background climate, we further evaluated a model combining radar backscatter, background climate, and dynamic climate variables (Rad-Clim_bg-dyn model). In the training dataset, performance metrics (R^2, RMSE, and BIC) were nearly identical to those of Rad-Clim_bg model, indicating no improvement during model fitting. In the validation and testing datasets, R^2 values of Rad-Clim_bg-dyn model

https://doi.org/10.5194/essd-2026-246
Preprint. Discussion started: 12 May 2026

Open Access Earth System Science Data Discussions

Table 1. Model predictors and model performance metrics: R^2, RMSE (Mg ha^{-1}), and BIC in training, validation, and testing dataset for random forest regression models of above-ground biomass.

Model	Predictor	R^2			RMSE (Mg ha^{-1})			BIC		
		Train	Validation	Test	Train	Validation	Test	Train	Validation	Test
Rad	[Rad]	0.884	0.175	0.136	31.3	83.3	85.2	9599995	3082066	5138267
Rad-Clim_bg	[Rad, MAT_bg, MAP_bg]	**0.977**	**0.815**	**0.833**	**14.0**	**39.4**	**37.5**	**7353055**	**2561017**	**4189492**
Rad-Clim_bg-dyn	[Rad, MAT_bg, MAP_bg, MAT_dyn, MAP_dyn]	0.977	0.787	0.662	13.8	42.4	53.3	7315772	2610684	4594888

were substantially higher than those of the Rad model (>0.66 vs. <0.20) but remained lower than those of Rad-Clim_bg model (>0.80). Similarly, RMSE and BIC were improved relative to Rad but were consistently worse than Rad-Clim_bg model.

Overall, the Rad-Clim_bg model achieved the best predictive performance, with the highest test R^2 (0.883), lowest test RMSE (37.5 Mg ha^{-1}), and lowest BIC. We therefore selected Rad-Clim_bg model as the final model for generating AGB estimates from 1993 to 2020.

We further evaluated our AGB product against independent field inventory measurements. Figure 1 compares inventory-derived AGB with (A) our product and (B–C) two widely used global satellite-derived AGB datasets. Our product shows moderate agreement with inventory data (R = 0.527), capturing mean AGB across grid cells but slightly overestimating high AGB values and underestimating low AGB values. Among the three satellite-derived products, our dataset exhibits the highest correlation with field measurements (Figure 1 A-C).

3.2 Spatial patterns of above-ground biomass carbon

From 1993 to 2020, our estimates reveal a mean global forest AGC density of 45.7 MgC ha^{-1}, with large regional variations (Figure 2 A): tropical forests exhibit the highest AGC densities (73.5 MgC ha^{-1}), followed by mid-latitude forests range from 27.7 to 46.4 MgC ha^{-1}. Interannual variability of AGC is high in arid and semi-arid regions, and low in humid areas with high biomass densities (Figure 2 B). The mean global forest above-ground biomass carbon stock during 1993–2020 is estimated at 191 $\pm$2.5 PgC. Tropical forests account for approximately 66% of global AGC stocks (127 PgC aggregated). Of this tropical total, 64.2 PgC (51%) located in South America (Figure 2 C). Tropical Africa stores 38.5 PgC, representing the second-largest tropical carbon pool. Although tropical Asia stores less carbon than tropical America and Africa, its stock remains larger than that of most non-tropical forest regions. Temperate and boreal forests store 20.7 PgC and 19.9 PgC of above-ground biomass carbon, respectively, while subtropical forests contribute approximately 10 PgC less than temperate forests.

https://doi.org/10.5194/essd-2026-246
Preprint. Discussion started: 12 May 2026

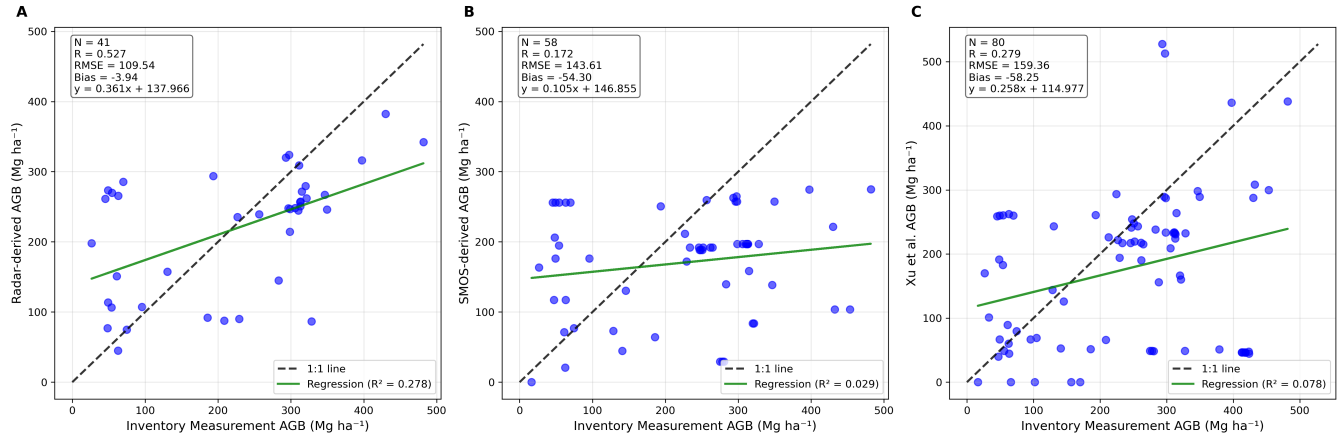

Figure 1. Comparison of satellite-derived above-ground biomass (AGB) estimates against plot inventory observations. (A) AGB estimates from satellite radar backscatter data (this study), (B) AGB estimates from SMOS VOD (Vegetation Optical Depth) dataset from Yang et al. (2023)), (C) AGB estimates from Xu et al. (2021) dataset.

3.3 Temporal changes in above-ground biomass carbon

From 1993 to 2020, AGC density exhibits a widespread increase globally in carbon density with spatially contrasting trends (Figure 3A). Approximately 58.6% of the forest land area exhibits increasing trends at an overall average trend of 0.42 MgC ha^{-1} yr^{-1}, primarily located in Southern Africa, Central Europe, the northeastern part of North America, and Southern China. Conversely, we find declining trends in Central and South America, Northeastern Europe, and Southeastern Russia, corresponding to 41.4% of the vegetated area, and an average rate of -0.39 MgC ha^{-1} yr^{-1}.

Consistent with this positive overall trend, the global mean aboveground biomass carbon shows a slight increase over 1993–2020, with an increase rate of 0.29 PgC yr^{-1} (Figure 3B). This net increase is underpinned by a mean decadal AGC stock change ranging from –0.74 to +1.02 PgC yr^{-1} (Figure 3B, grey bars). In regions with positive AGC trends (Figure 3A), we estimate a gross AGC gain of ca. 20 PgC from 1993 to 2020, with a mean carbon gain rate of 0.84 PgC yr^{-1} (Figure 3C). These carbon gains are supported by the strong increasing decadal AGC stock change rate, from a mean net AGC stock change in aboveground biomass of about 0.82 PgC yr^{-1} in 1990s to 1.02 PgC yr^{-1} in 2010s (Figure 3C). In contrast, regions with declining AGC trends (Figure 3D) experienced a gross loss of 12 PgC, driven by persistent carbon emissions (e.g., -0.74 PgC yr^{-1} in 2000s). These two contrasting trends result in a net sink in aboveground biomass of 0.44 PgC yr^{-1} (Figure 3B).

The interannual variability in AGC stock also differ widely across biomes (Figure 4). Global tropical forests exhibit a net carbon stock increase over 1993–2020 (Figure 4A). However, this aggregate change shows substantial regional variability. Tropical Africa experienced significant carbon increase during 2000–2009 (0.22 PgC yr^{-1}), continuing into 2010–2019 (0.08 PgC yr^{-1}) (Figure 4C). Tropical America and tropical Asia show more recent declines. In tropical America, AGC stock decline intensified after 2000, increasing from –0.06 PgC yr^{-1} during 2000–2009 to –0.12 PgC yr^{-1} thereafter (Figure 4B). In tropical Asia, AGC declines became evident primarily after 2010.

https://doi.org/10.5194/essd-2026-246
Preprint. Discussion started: 12 May 2026

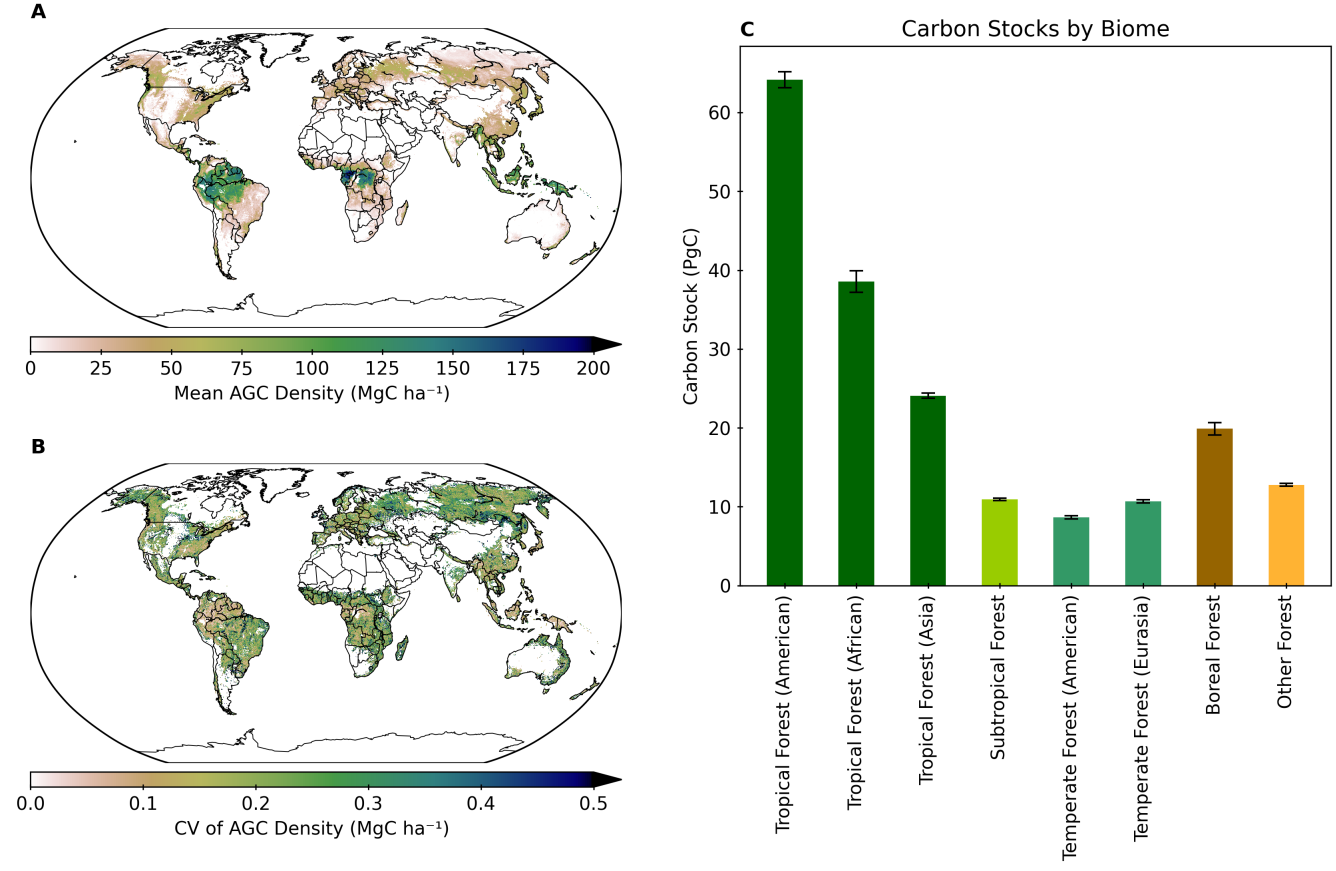

Figure 2. Mean above-ground biomass carbon (AGC) density and stocks from 1993 to 2020. (A) Spatial distribution of mean global above-ground carbon density and (B) corresponding CV (coefficient of variation). (C) Above-ground biomass carbon stocks aggregated for global biomes. Black error bars represent the standard deviation of AGC stocks for each biome.

In contrast, subtropical, temperate, and boreal forests contributed predominantly to global carbon gains. Subtropical forests experienced declines in the first decade of the study period but shifted to carbon gains after 2000, with a mean AGC stock increase of 0.02 PgC yr^{-1} (Figure 4E). Global temperate forests show increasing AGC trends, particularly after 2002, with a gross gain of 1.14 PgC over the study period (Figure 4F). Boreal forests generally acted as a carbon sink from 1993 to 2020, with the mean decadal AGC stock change increase rising from 0.09 PgC yr^{-1} to 0.14 PgC yr^{-1} (Figure 4G). Other forest biomes exhibited relatively stable AGC stocks with low variability throughout the study period (Figure 4H).

4 Discussion

In our study, we generated a new long-term, moderate-resolution above-ground biomass dataset derived from satellite radar backscatter. The dataset provides continuous above-ground biomass estimations over approximately 30 years from 1993 to

https://doi.org/10.5194/essd-2026-246
Preprint. Discussion started: 12 May 2026

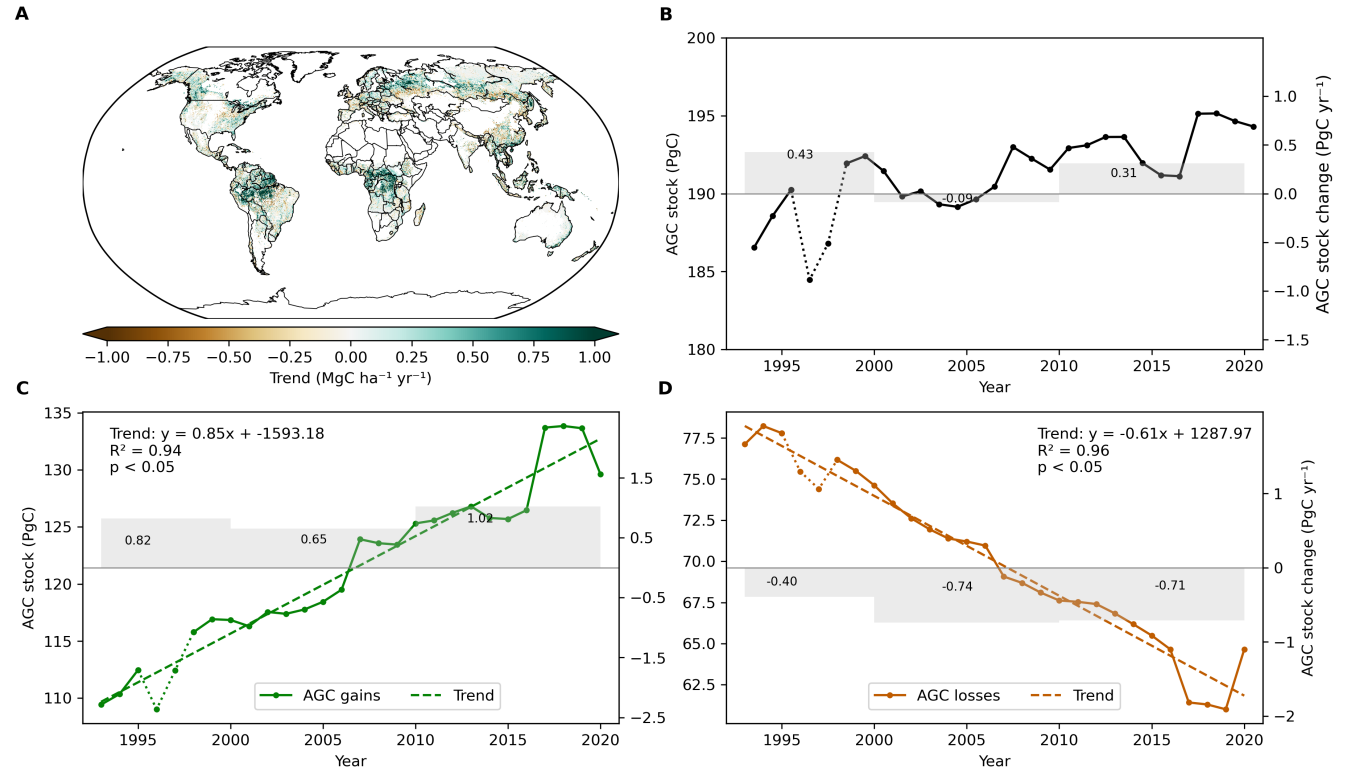

Figure 3. Trend in global above-ground biomass carbon during 1993 to 2020. (A) Global forest AGC density trend map. (B) Interannual changes in global annual forest AGC stock (left y-axis) and mean decadal AGC stock change (grey bar, right y-axis). (C) Changes in annual AGC stock (left y-axis) and mean decadal AGC stock change (grey bar, right y-axis) in regions with increasing trends of AGC. (D) Changes in annual AGC stock (left y-axis) and mean decadal AGC stock change (grey bar, right y-axis) in regions with decreasing trends of AGC. AGC stock change values are displayed adjacent to the grey bars. Dashed lines in (C) and (D) represent trend lines for annual carbon stock changes, with trend equations, R^2, and p-values provided. Dotted lines in 1997 highlight estimates that may be affected by unreliable radar scatter data quality.

https://doi.org/10.5194/essd-2026-246
Preprint. Discussion started: 12 May 2026

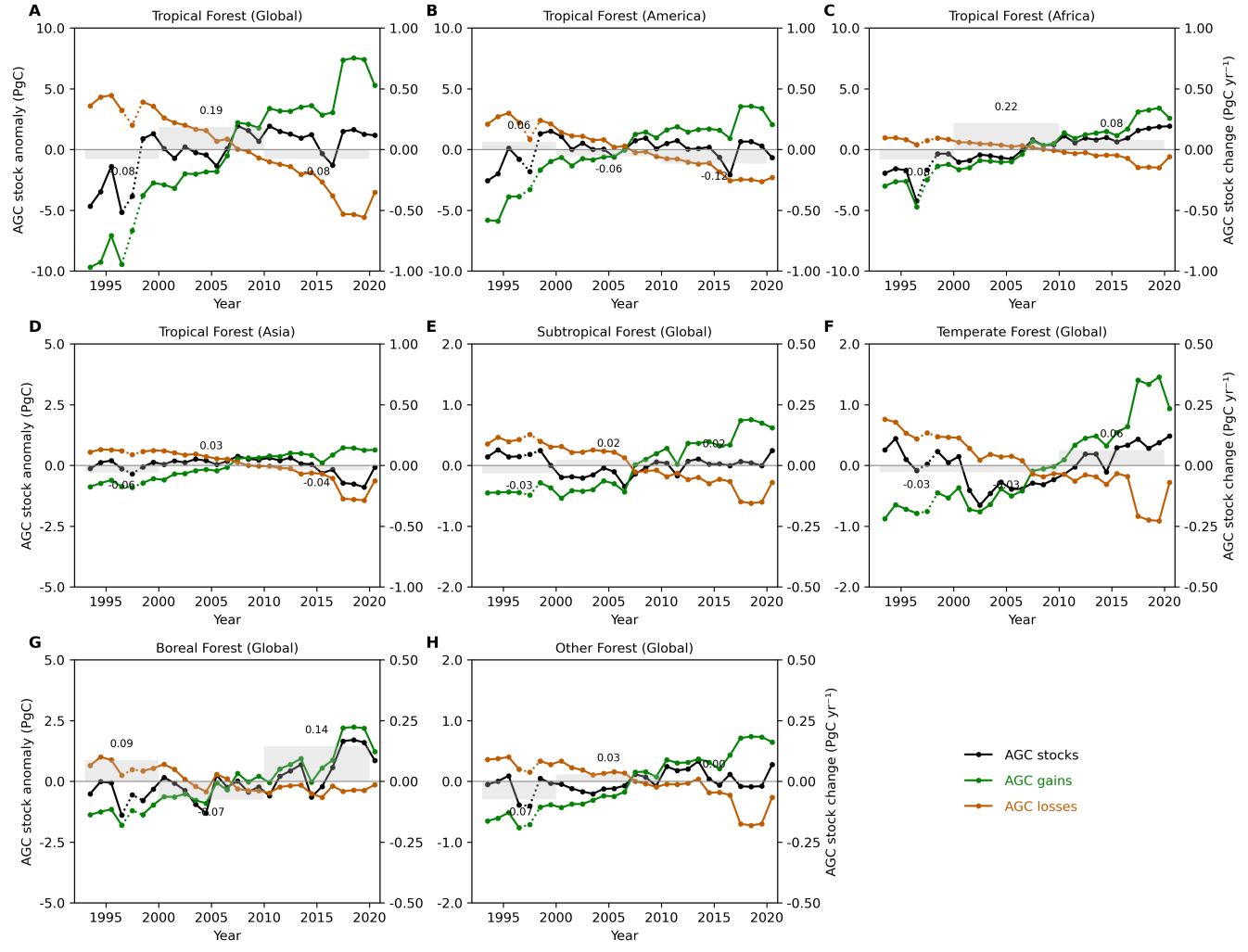

Figure 4. Temporal patterns of annual anomalies in AGC stocks (black line), carbon gains (green line, representing regions with increasing above-ground biomass trends), carbon losses (brown line, representing regions with decreasing above-ground biomass trends), and mean decadal AGC stock change (grey bar) for each biome. AGC stock change values are displayed adjacent to the grey bars. Dotted lines around 1997 highlight estimates that may be affected by unreliable radar backscatter data quality.

https://doi.org/10.5194/essd-2026-246
Preprint. Discussion started: 12 May 2026

2020, making it the longest temporally consistent global biomass records currently available. Furthermore, the spatial resolution (8.9 km) is substantially finer than that of long-term vegetation optical depth (VOD)-based products (25 km), enabling improved detection of regional biomass variability (Liu et al., 2015; Fan et al., 2019; Yang et al., 2023). Most existing long-term biomass datasets rely on VOD retrievals from passive microwave sensors and empirical relationships calibrated against satellite biomass maps at continental scales (Fan et al., 2019; Yang et al., 2023). In contrast, we employed a global machine learning approach that integrates radar backscatter with background climate variables. This strategy allows the model to account for regional differences in the radar–biomass relationship (e.g., semi-arid versus humid tropical systems).

4.1 Comparison with other above-ground biomass datasets

4.1.1 Field inventory above-ground biomass measurements

Our AGB estimates show moderate agreement with independent plot-level field inventory measurements, with a Pearson correlation between our predictions and measurements of 0.53, root mean square error of 109.5 Mg ha^{-1} and a slope of the regression of 0.36 (Figure 1 A). Specifically, our dataset overestimates AGB in the lower ranges (<100 Mg ha^{-1}) and underestimates in the intermediate range between 100–300 Mg ha^{-1}. Nevertheless, our dataset outperforms two widely used satellite-derived datasets (Figure 1 B, C). Several factors likely explain the remaining discrepancies. First, inventory AGB is derived from individual tree measurements, whereas satellite AGB represents spatial averages at the pixel scale. To reduce scale mismatch, we restricted comparisons to pixels containing at least 10 inventory plots; however, structural differences between plot-level and gridded estimates inevitably introduce bias. Second, inventory datasets used here were compiled from published studies, limiting spatial coverage because most field inventory biomass data are not publicly accessible. Expanded access to harmonized global inventory datasets will be critical for more robust validation in the future.

4.1.2 Comparison in the spatial patterns of global above-ground biomass

Compared for the same reference period, same biomass carbon (AGC or TGC stock), same vegetation type (forest) and same spatial coverage, our estimates of mean global forest AGC stock is, as expected, very similar to ESA-CCI estimates. It is broadly consistent with other previous global assessments based on (Table 2), although slightly higher than the estimate by Yang et al. (2023) (AGC difference of 44.15 PgC) and Xu et al. (2021) (TGC difference of 4.13) and lower than Santoro et al. (2021) (AGC difference of -24.40 PgC). Compared to inventory estimates by Pan et al. (2024), our TGC estimates are slightly smaller, with a mean underestimation of 60.40–73.54 PgC, depending on the period considered. Potential reasons for the discrepancies with inventory lie on the different spatial resolution of each dataset, uncertainties in our approach to derive TGC from AGB, as well as in the differences in forest area considered. The forest area considered here excludes wetlands, barren land, regions with more than 10% peatland cover, and urban areas. In contrast, the inventory-based estimates encompass all forest areas, which likely contributes to the higher values reported in the inventory.

Despite differences in magnitude, the spatial distribution of biomass is consistent across datasets 1) Santoro et al. (2021), 2) Xu et al. (2021), 3) SMOS, estimates from Yang et al. (2023)): tropical forests contain the highest AGC densities globally,

https://doi.org/10.5194/essd-2026-246
Preprint. Discussion started: 12 May 2026

Open Access Earth System Science Data Discussions

Table 2. Comparison of global mean above-ground biomass carbon stocks between our product and other existing products. Note: The global mean above-ground biomass carbon stock for products marked with * is calculated based on the overlapping area between those products and our study area. Values for other products are taken directly from their respective publications.

Dataset	Variable	Period	Global (PgC)	This Study (PgC)	Difference (PgC)
ESA-CCI (*)	**AGC**	2017	191.28	191.30	0.02
		2018	191.30	191.50	0.20
		2019	191.05	191.08	0.03
		2020	190.54	190.21	-0.33
		2017-2020	191.05	191.03	-0.02
Santoro et al., 2021 (*)	**AGC**	1993-2019	215.53	191.13	-24.40
Yang et al., 2023 (*)	**AGC**	2010-2020	128.70	172.84	44.14
Xu et al., 2021 (*)	**TGC**	2000-2019	227.98	232.11	4.13
Pan et al., 2024	**TGC**	1990	301.40	227.86	-73.54
		2000	294.80	231.10	-63.70
		2010	297.30	234.37	-62.93
		2020	295.30	234.90	-60.40

followed by temperate and boreal systems (Figure S4). Agreement in large-scale spatial patterns suggests robust representation of first-order biomass gradients across independent products.

4.1.3 Comparison in the temporal pattern of global above-ground biomass

Our analysis of AGC changes between 1993 and 2020 reveals a slight increase of global AGC stock dynamics (Figure 3). Globally, we observed two contrasting trends in gross changes (carbon gains and carbon losses) during 1993–2020, leading to a small net carbon sink in above-ground biomass globally. This suggests that carbon gains, likely associated with longer growing seasons (Piao et al., 2007) and elevated CO_2 effects (Walker et al., 2021) slightly outweighed the negative effects of carbon losses from climatic extremes (Yang et al., 2018), natural disturbances (Harris et al., 2016) and land-use changes (Winkler et al., 2023) during the study period and study forest areas. This finding aligns with recent field inventory-based studies, such as Pan et al. (2024), which report consistent carbon sinks across global forest ecosystems over the past 30 years.

We further compared net annual TGC changes (PgC yr^{-1}; given most datasets report TGC rather than AGC) from 2010 to 2019 globally and across three climate zones (tropical, temperate, and boreal) with other global estimates (Table 3). Our global estimate of net TGC change is 0.40 PgC yr^{-1}, identical to the evaluate by Bar-On et al. (2025). It indicates a net biomass carbon sink, though it is lower than values reported by Xu et al. (2021) (0.56 PgC yr^{-1}), Yang et al. (2023) (0.50 PgC yr^{-1}), and Pan et al. (2024) (0.99 PgC yr^{-1}). By zone, tropical forests show a slight net loss of 0.02 PgC yr^{-1}, consistent with Yang et al. (2023) (-0.08 PgC yr^{-1}) and Xu et al. (2026) (-0.09 PgC yr^{-1}). In contrast, Xu et al. (2021) and Pan et al. (2024) reported a carbon gain of 0.16 PgC yr^{-1} and 0.28 PgC yr^{-1} respectively, for tropical forests over 2010-2019. Temperate forests exhibit

https://doi.org/10.5194/essd-2026-246
Preprint. Discussion started: 12 May 2026

Open Access Earth System Science Data Discussions

Table 3. The net total living biomass carbon (TGC) changes (PgC yr^{-1}) from 2010 to 2019 globally and for three biomes (tropical, temperate and boreal forest). TGC changes reported from Bar-On et al. (2025) covers 2011-2019, and from Xu et al. (2026) covers 1990-2020. TGC in Xu et al. (2026) was derived from AGC. TGC changes from Pan et al. (2024) for global and tropical forests were estimated from net forest carbon change, apportioned by the fractional contribution of total living biomass.

Dataset	Global	Tropical Forest	Temperate Forest	Boreal Forest
This study	0.40	-0.02	0.12	0.33
Xu et al., 2021	0.56	0.16	0.23	0.17
Yang et al., 2023	0.50	-0.08	0.13	0.37
Bar-on et al., 2025	0.40 (2011-2019)	/	/	/
Xu et al., 2026	/	-0.09 (1990-2020)	/	/
Pan et al., 2024	0.99	0.28	0.47	0.04

a net biomass carbon gain (0.12 PgC yr^{-1}), similar to Yang et al. (2023) (0.13 PgC yr^{-1}) and lower than the values reported by Xu et al. (2021) (0.23 PgC yr^{-1}) and Pan et al. (2024) (0.47 PgC yr^{-1}). For boreal forests, our estimate of 0.33 PgC yr^{-1} is comparable to that of Yang et al. (2023) (0.37 PgC yr^{-1}), but higher than Xu et al. (2021) (0.17 PgC yr^{-1}) and Pan et al. (2024) (0.04 PgC yr^{-1}).

Regionally, tropical Africa forest, subtropical, temperate and boreal forests dominate global AGC gains from 1993 to 2020 (Figure 4). Despite AGC declines in the early decade for subtropical and temperate forests, AGC stock loss change to AGC gain. These increase in AGC is supported by forest area expansion and improved forest management, longer growing seasons, CO_2 fertilization (Myneni et al., 2001; Erb et al., 2018; Etzold et al., 2020; Ameray et al., 2021; Yao et al., 2024). Boreal forests functioned as a net carbon sink during 1993-2020, but in 2000-2009, it shows a bit decrease with the carbon sink of -0.07 PgC yr^{-1}. This might be correlated with increasing climate sensitivity of boreal ecosystems (Eckdahl et al., 2022) and rising disturbance pressure from fires, logging, and extreme events (Mack et al., 2021; Wang et al., 2021; Shvetsov et al., 2021; Kwon et al., 2021). Despite declines in the decades of our study period, boreal forests remain a net carbon sink over the full study periods, consistent with other studies (Xu et al., 2021; Yang et al., 2023; Pan et al., 2024).

Tropical forests in American and Asia, in contrast, are the primary contributors to global above-ground biomass carbon losses. Tropical America shows the decline in recent two decades, consistent with evidence for the weak carbon sink in tropics (Brienen et al., 2015; Baccini et al., 2017; Hubau et al., 2020). These losses are associated with deforestation, forest degradation, drought-induced mortality, and slowing growth rates (Phillips et al., 2009; Lewis et al., 2011; Hubau et al., 2020; Gatti et al., 2021; Qin et al., 2021), as evidenced by negative AGC trends in the arc of deforestation (Figure 3). Our results support growing evidence that parts of the Amazon are transitioning toward a reduced or neutral carbon sink (Fawcett et al., 2023; Uribe et al., 2023; Pan et al., 2024), at least in the aboveground components. Tropical Asia exhibit smaller declines, particularly after 2010. These trends are consistent with ongoing land-use change, including agricultural expansion and plantation development (Tyukavina et al., 2018; Feng et al., 2022; Vijay et al., 2016).These losses may become increasingly important under continued deforestation and climate stress.

https://doi.org/10.5194/essd-2026-246
Preprint. Discussion started: 12 May 2026

4.2 Uncertainty and limitation of our global above-ground biomass dataset

Despite the overall robustness of our dataset, several sources of uncertainty remain. These primarily arise from input data quality, the machine learning model, and limitations in spatial and temporal generalization. Uncertainty in the input radar backscatter data represents a major source of potential bias. The radar record integrates observations from multiple satellite sensors with differing instrument characteristics, which may introduce inconsistencies over time. A notable example occurs around 1997, when our dataset shows a sharp decline in AGC followed by rapid recovery in 1998 (Figure 3B). Accordingly, biomass estimates for 1997 should be interpreted with caution. In addition, our dataset is derived from C-band radar observations. While widely used for vegetation monitoring (Besnard et al., 2021; Santoro et al., 2021), C-band signals are primarily sensitive to upper canopy structure. As a result, lower canopy and woody components may be underrepresented, potentially leading to underestimation of total biomass in dense forests.

Our machine learning model was trained using the ESA-CCI above-ground biomass product as the reference target. Although ESA-CCI is one of the most widely used global biomass datasets, it contains its own uncertainties arising from sensor limitations, retrieval algorithms, and spatial heterogeneity in calibration data. These uncertainties are inevitably propagated into our model. Model-derived uncertainty is generally low but spatially heterogeneous, with higher uncertainty in boreal Eurasia and parts of tropical Africa, South America, and Southeast Asia. These regions combine high biomass density with complex forest structure, which challenges radar-based retrievals. Our global above-ground biomass estimates are derived from the random forest regression models using radar scatter data, along with additional climate and forest structure predictors. While the models exhibit generally low mean uncertainty in global vegetation AGC predictions (Figure 5), indicating stable predictions across models trained in each cross-validation, regional variations exist. Higher uncertainties are observed in western and central Russian boreal forests, southeastern Asian tropical forests, and parts of tropical Africa and South America. Despite these localized uncertainties, the absolute AGC in these regions remains high, resulting in relatively low proportional uncertainty. One key source of uncertainty stems from the random forest regression models themselves. We employed a spatiotemporal block cross-validation approach to ensure robust wall-to-wall estimation of AGC from radar backscatter data. Although this method improves model generalizability, it does not fully account for uncertainties arising from regional variability in forest structure and environmental conditions.

Our dataset provides biomass estimates at a spatial resolution of 8.9 km, which is determined by the radar backscatter record used as predictors. Notably, 8.9 km is currently higher than the nominal resolution of the radar backscatter data (typically 50 km or 25 km). Although higher-resolution biomass products already exist (e.g., the 100 m ESA CCI biomass maps), they are available only for a few discrete years or short recent periods (e.g., 2007, 2010, and 2015–2022). Using these snapshots to infer annual biomass dynamics would require space-for-time substitution, a method that can misrepresent temporal change and introduce substantial uncertainty. In contrast, our 8.9 km product provides annually consistent, globally complete estimates from the 1990s through 2020, enabling direct tracking of biomass change over time. The trade-off is reduced spatial detail: small or sub-pixel disturbances such as selective logging or narrow clearings may not be detectable if they affect only a minor fraction of an 8.9 km pixel. For applications focused on fine-scale features, we recommend pairing our temporally

https://doi.org/10.5194/essd-2026-246
Preprint. Discussion started: 12 May 2026

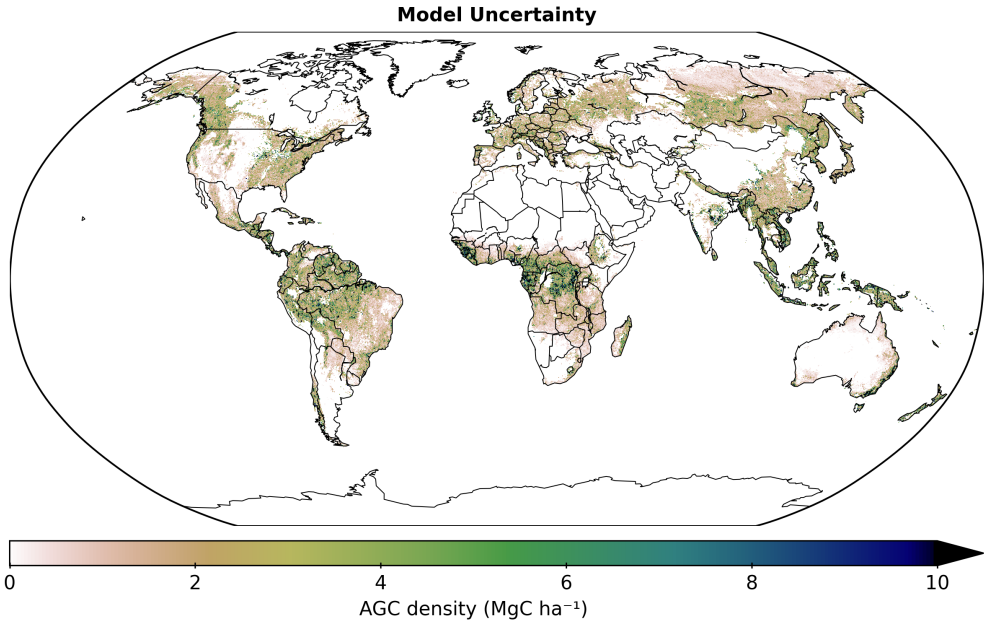

Figure 5. Model uncertainty for predicting above-ground biomass carbon

consistent record with higher-resolution biomass or disturbance layers to identify local impacts, while acknowledging the added uncertainty that comes with extrapolating those high-resolution snapshots across multiple years.

4.3 Advantages of our global dynamical above-ground biomass dataset

Our dataset offers several key advantages for studying biomass dynamics. First, its long temporal coverage enables direct observation of biomass changes, avoiding assumptions inherent in space-for-time substitution approaches (Pickett, 1989). Such approaches assume spatial gradients represent temporal trajectories, which may not hold under heterogeneous environmental conditions (e.g., soil type, climate) and disturbance regimes. By providing continuous temporal observations, our dataset allows more reliable attribution of above-ground biomass carbon dynamics.

Second, the dataset facilitates improved understanding of complex impacts of climate change and disturbances on carbon dynamics. Climate change, along with increased ecosystem disturbances, is expected to produce more intricate carbon dynamics, particularly at regional and local scales (Franklin et al., 2016; Dye et al., 2024). For example, increasing droughts not only directly affect but also legacy effects on ecosystem carbon changes (Fleta-Soriano and Munné-Bosch, 2016; Kannenberg et al., 2020; Xu et al., 2021). Droughts can also trigger further disturbances, such as fires and insect outbreaks, thereby compounding stress on vegetation which lead to more tree mortality (Allen et al., 2010; Seidl et al., 2011; Anderegg et al., 2015; Burton et al., 2020). An increase in drought-induced tree mortality has been reported (Hammond et al., 2022), but remains challenging to detect in remote-sensing observations and to simulate in models (Hartmann et al., 2022). Additionally, human activities such as

https://doi.org/10.5194/essd-2026-246
Preprint. Discussion started: 12 May 2026

land-use change and management (Houghton, 2003; Lai et al., 2016) further complicate carbon dynamics. A major limitation in understanding of biomass changes in response to these extremes and disturbances is the fact that AGB datasets tend to be short-term or discrete, while understanding biomass losses from extremes, forest degradation and tree mortality, as well as recovery dynamics, require spatially and temporally continuous long-term datasets (Bustamante et al., 2016; Fu et al., 2017; Matricardi et al., 2020; Hartmann et al., 2022). Moreover, the disturbances often occuring at small spatial scales (25-100 m), require a pixel size close to the disturbance size (Houghton et al., 2009). our dataset, while relatively coarse compared to the finest disturbance scales, remains the highest spatial resolution available for dynamical AGB datasets. This resolution enables better detection of regional disturbance signals and supports more detailed attribution studies at continental scales.

Finally, the dataset has potential to improve land surface and Earth system modeling. Many models poorly represent biomass mortality, disturbance dynamics, and land-use effects due to limited observational constraints (Seidl et al., 2011; Manusch et al., 2012; Pongratz et al., 2018; Pugh et al., 2019; Yang et al., 2020a; El Masri and Xiao, 2025). By providing temporally continuous biomass estimates, our dataset can help constrain model parameterizations, reduce uncertainties in simulated carbon sinks, and reconcile discrepancies between observation-based and model-based carbon budgets.

5 Conclusion

We developed a new long-term, moderate-resolution global forest above-ground biomass dataset derived from satellite radar backscatter using a machine learning framework. Incorporating background climate variables substantially improves biomass estimation compared with radar-only models, whereas dynamic climate predictors do not provide additional predictive skill. Our analysis reveals a slight increase in global carbon stocks, characterized by a dynamic balance between AGC gains and losses across different biomes. Temperate, boreal and tropical Africa forests are the primary contributors to AGC gains, while AGC losses are predominantly observed in tropical America and Asia forests, particularly in South America. This dataset provides new opportunities to investigate the impacts of climate variability, disturbances, and land-use change on global biomass dynamics. It also offers valuable constraints for improving the representation of biomass processes in Earth system models, thereby reducing uncertainties in future carbon cycle projections.

Code and data availability. The global above-ground biomass dataset at 8.9 km resolution from 1993 to 2020 is openly available on Zenodo: https://zenodo.org/records/19259660 (Liu et al., 2026). The corresponding modeling code is publicly hosted on GitHub: https://github.com/Guohua-liu/CALIPSO_Biomass/tree/main/AGB_Mapping/scripts.

Author contributions. G.L. and A.B. conceived the research and G.L. performed all analyses with support by A.B.. S.T. and C.X. provided support on satellite radar backscatter data analysis, and H.Y. prepared the biomass data from SMOS-IC L-VOD data. G.L. performed data processing and interpretation of results with support by A.B.. G.L. and A.B. prepared the draft of the manuscript. P.C. provided expertise on biomass modeling. All authors contributed to revisions of the manuscript and approved the final version.

https://doi.org/10.5194/essd-2026-246
Preprint. Discussion started: 12 May 2026

Open Access Earth System Science Data Discussions

Competing interests. The authors declare no competing interests.

Acknowledgements. We thank support from the CALIPSO (Carbon Loss in Plant Soils and Oceans) project, funded through the generosity of Eric and Wendy Schmidt by recommendation of the Schmidt Futures program. A.B. acknowledges support from the European Union (ERC StG, ForExD, Grant No. 101039567). We thank Ulrich Weber (MPI-BGC) for data downloading and aggregation.

https://doi.org/10.5194/essd-2026-246
Preprint. Discussion started: 12 May 2026

Open Access Earth System Science Data Discussions

References

Abatzoglou, J. T., Dobrowski, S. Z., Parks, S. A., and Hegewisch, K. C.: TerraClimate, a high-resolution global dataset of monthly climate and climatic water balance from 1958–2015, Scientific data, 5, 1–12, 2018.

Ahlström, A., Schurgers, G., and Smith, B.: The large influence of climate model bias on terrestrial carbon cycle simulations, Environmental Research Letters, 12, 014 004, 2017.

Allen, C. D., Macalady, A. K., Chenchouni, H., Bachelet, D., McDowell, N., Vennetier, M., Kitzberger, T., Rigling, A., Breshears, D. D., Hogg, E. T., et al.: A global overview of drought and heat-induced tree mortality reveals emerging climate change risks for forests, Forest ecology and management, 259, 660–684, 2010.

Ameray, A., Bergeron, Y., Valeria, O., Montoro Girona, M., and Cavard, X.: Forest carbon management: A review of silvicultural practices and management strategies across boreal, temperate and tropical forests, Current Forestry Reports, pp. 1–22, 2021.

Anderegg, W. R., Hicke, J. A., Fisher, R. A., Allen, C. D., Aukema, J., Bentz, B., Hood, S., Lichstein, J. W., Macalady, A. K., McDowell, N., et al.: Tree mortality from drought, insects, and their interactions in a changing climate, New Phytologist, 208, 674–683, 2015.

Anderson-Teixeira, K. J., Wang, M. M., McGarvey, J. C., Herrmann, V., Tepley, A. J., Bond-Lamberty, B., and LeBauer, D. S.: ForC: a global database of forest carbon stocks and fluxes., Ecology, 99, 2018.

Baccini, A., Goetz, S., Walker, W., Laporte, N., Sun, M., Sulla-Menashe, D., Hackler, J., Beck, P., Dubayah, R., Friedl, M., et al.: Estimated carbon dioxide emissions from tropical deforestation improved by carbon-density maps, Nature climate change, 2, 182–185, 2012.

Baccini, A., Walker, W., Carvalho, L., Farina, M., Sulla-Menashe, D., and Houghton, R.: Tropical forests are a net carbon source based on aboveground measurements of gain and loss, Science, 358, 230–234, 2017.

Bar-On, Y. M., Li, X., O'sullivan, M., Wigneron, J.-P., Sitch, S., Ciais, P., Frankenberg, C., and Fischer, W. W.: Recent gains in global terrestrial carbon stocks are mostly stored in nonliving pools, Science, 387, 1291–1295, 2025.

Bastos, A., Ciais, P., Sitch, S., Aragão, L. E. O. C., Chevallier, F., Fawcett, D., Rosan, T. M., Saunois, M., Günther, D., Perugini, L., Robert, C., Deng, Z., Pongratz, J., Ganzenmüller, R., Fuchs, R., Winkler, K., Zaehle, S., and Albergel, C.: On the use of Earth Observation to support estimates of national greenhouse gas emissions and sinks for the Global stocktake process: lessons learned from ESA-CCI RECCAP2, Carbon Balance and Management, 17, 15, https://doi.org/10.1186/s13021-022-00214-w, 2022.

Beer, C., Reichstein, M., Tomelleri, E., Ciais, P., Jung, M., Carvalhais, N., Rödenbeck, C., Arain, M. A., Baldocchi, D., Bonan, G. B., et al.: Terrestrial gross carbon dioxide uptake: global distribution and covariation with climate, Science, 329, 834–838, 2010.

Besnard, S., Santoro, M., Cartus, O., Fan, N., Linscheid, N., Nair, R., Weber, U., Koirala, S., and Carvalhais, N.: Global sensitivities of forest carbon changes to environmental conditions, Global Change Biology, 27, 6467–6483, 2021.

Bonan, G. B.: Forests and climate change: forcings, feedbacks, and the climate benefits of forests, science, 320, 1444–1449, 2008.

Brienen, R. J., Phillips, O. L., Feldpausch, T. R., Gloor, E., Baker, T. R., Lloyd, J., Lopez-Gonzalez, G., Monteagudo-Mendoza, A., Malhi, Y., Lewis, S. L., et al.: Long-term decline of the Amazon carbon sink, Nature, 519, 344–348, 2015.

Burton, P. J., Jentsch, A., and Walker, L. R.: The ecology of disturbance interactions, BioScience, 70, 854–870, 2020.

Bustamante, M. M., Roitman, I., Aide, T. M., Alencar, A., Anderson, L. O., Aragão, L., Asner, G. P., Barlow, J., Berenguer, E., Chambers, J., et al.: Toward an integrated monitoring framework to assess the effects of tropical forest degradation and recovery on carbon stocks and biodiversity, Global change biology, 22, 92–109, 2016.

https://doi.org/10.5194/essd-2026-246
Preprint. Discussion started: 12 May 2026

Dye, A. W., Houtman, R. M., Gao, P., Anderegg, W. R., Fettig, C. J., Hicke, J. A., Kim, J. B., Still, C. J., Young, K., and Riley, K. L.: Carbon, climate, and natural disturbance: a review of mechanisms, challenges, and tools for understanding forest carbon stability in an uncertain future, Carbon Balance and Management, 19, 1–25, 2024.

Eckdahl, J. A., Kristensen, J. A., and Metcalfe, D. B.: Climatic variation drives loss and restructuring of carbon and nitrogen in boreal forest wildfire, Biogeosciences, 19, 2487–2506, 2022.

El Masri, B. and Xiao, J.: Comparison of global aboveground biomass estimates from satellite observations and dynamic global vegetation models, Journal of Geophysical Research: Biogeosciences, 130, e2024JG008 305, 2025.

El-Masri, B., Barman, R., Meiyappan, P., Song, Y., Liang, M., and Jain, A. K.: Carbon dynamics in the Amazonian Basin: Integration of eddy covariance and ecophysiological data with a land surface model, Agricultural and forest meteorology, 182, 156–167, 2013.

Erb, K.-H., Kastner, T., Plutzar, C., Bais, A. L. S., Carvalhais, N., Fetzel, T., Gingrich, S., Haberl, H., Lauk, C., Niedertscheider, M., et al.: Unexpectedly large impact of forest management and grazing on global vegetation biomass, Nature, 553, 73–76, 2018.

Etzold, S., Ferretti, M., Reinds, G. J., Solberg, S., Gessler, A., Waldner, P., Schaub, M., Simpson, D., Benham, S., Hansen, K., et al.: Nitrogen deposition is the most important environmental driver of growth of pure, even-aged and managed European forests, Forest Ecology and Management, 458, 117 762, 2020.

Fan, L., Wigneron, J.-P., Ciais, P., Chave, J., Brandt, M., Fensholt, R., Saatchi, S. S., Bastos, A., Al-Yaari, A., Hufkens, K., et al.: Satellite-observed pantropical carbon dynamics, Nature plants, 5, 944–951, 2019.

Fan, L., Wigneron, J.-P., Ciais, P., Chave, J., Brandt, M., Sitch, S., Yue, C., Bastos, A., Li, X., Qin, Y., et al.: Siberian carbon sink reduced by forest disturbances, Nature Geoscience, 16, 56–62, 2023.

Fan, L., Cui, T., Wigneron, J.-P., Ciais, P., Sitch, S., Brandt, M., Li, X., Niu, S., Xiao, X., Chave, J., et al.: Dominant role of the non-forest woody vegetation in the post 2015/16 El Niño tropical carbon recovery, Global Change Biology, 30, e17 423, 2024.

Fang, H., Fan, L., Ciais, P., Xiao, J., Fensholt, R., Chen, J., Frappart, F., Ju, W., Niu, S., Xiao, X., et al.: Satellite-based monitoring of China's above-ground biomass carbon sink from 2015 to 2021, Agricultural and Forest Meteorology, 356, 110 172, 2024.

Fawcett, D., Sitch, S., Ciais, P., Wigneron, J. P., Silva-Junior, C. H., Heinrich, V., Vancutsem, C., Achard, F., Bastos, A., Yang, H., et al.: Declining Amazon biomass due to deforestation and subsequent degradation losses exceeding gains, Global Change Biology, 29, 1106–1118, 2023.

Feng, Y., Zeng, Z., Searchinger, T. D., Ziegler, A. D., Wu, J., Wang, D., He, X., Elsen, P. R., Ciais, P., Xu, R., et al.: Doubling of annual forest carbon loss over the tropics during the early twenty-first century, Nature Sustainability, 5, 444–451, 2022.

Feng, Y., Ciais, P., Wigneron, J.-P., Xu, Y., Ziegler, A. D., van Wees, D., Fendrich, A. N., Spracklen, D. V., Sitch, S., Brandt, M., et al.: Global patterns and drivers of tropical aboveground carbon changes, Nature Climate Change, 14, 1064–1070, 2024.

Fleta-Soriano, E. and Munné-Bosch, S.: Stress memory and the inevitable effects of drought: a physiological perspective, Frontiers in Plant Science, 7, 143, 2016.

Frank, D., Reichstein, M., Bahn, M., Thonicke, K., Frank, D., Mahecha, M. D., Smith, P., Van der Velde, M., Vicca, S., Babst, F., et al.: Effects of climate extremes on the terrestrial carbon cycle: concepts, processes and potential future impacts, Global change biology, 21, 2861–2880, 2015.

Franklin, J., Serra-Diaz, J. M., Syphard, A. D., and Regan, H. M.: Global change and terrestrial plant community dynamics, Proceedings of the National Academy of Sciences, 113, 3725–3734, 2016.

Friedlingstein, P., O'sullivan, M., Jones, M. W., Andrew, R. M., Bakker, D. C., Hauck, J., Landschützer, P., Le Quéré, C., Luijkx, I. T., Peters, G. P., et al.: Global carbon budget 2023, Earth System Science Data, 15, 5301–5369, 2023.

https://doi.org/10.5194/essd-2026-246
Preprint. Discussion started: 12 May 2026

Friend, A. D., Lucht, W., Rademacher, T. T., Keribin, R., Betts, R., Cadule, P., Ciais, P., Clark, D. B., Dankers, R., Falloon, P. D., et al.: Carbon residence time dominates uncertainty in terrestrial vegetation responses to future climate and atmospheric CO2, Proceedings of the National Academy of Sciences, 111, 3280–3285, 2014.

Fu, Z., Li, D., Hararuk, O., Schwalm, C., Luo, Y., Yan, L., and Niu, S.: Recovery time and state change of terrestrial carbon cycle after disturbance, Environmental Research Letters, 12, 104 004, 2017.

Gatti, L. V., Basso, L. S., Miller, J. B., Gloor, M., Gatti Domingues, L., Cassol, H. L., Tejada, G., Aragão, L. E., Nobre, C., Peters, W., et al.: Amazonia as a carbon source linked to deforestation and climate change, Nature, 595, 388–393, 2021.

Gibbs, H. K. and Ruesch, A.: New IPCC tier-1 global biomass carbon map for the year 2000, Tech. rep., Environmental System Science Data Infrastructure for a Virtual Ecosystem, 2008.

Hammond, W. M., Williams, A. P., Abatzoglou, J. T., Adams, H. D., Klein, T., López, R., Sáenz-Romero, C., Hartmann, H., Breshears, D. D., and Allen, C. D.: Global field observations of tree die-off reveal hotter-drought fingerprint for Earth's forests, Nature Communications, 13, 1761, 2022.

Harper, K. L., Lamarche, C., Hartley, A., Peylin, P., Ottlé, C., Bastrikov, V., San Martín, R., Bohnenstengel, S. I., Kirches, G., Boettcher, M., et al.: A 29-year time series of annual 300 m resolution plant-functional-type maps for climate models, Earth System Science Data, 15, 1465–1499, 2023.

Harris, N., Hagen, S., Saatchi, S., Pearson, T., Woodall, C., Domke, G., Braswell, B., Walters, B., Brown, S., Salas, W., et al.: Attribution of net carbon change by disturbance type across forest lands of the conterminous United States, Carbon balance and management, 11, 1–21, 2016.

Hartmann, H., Bastos, A., Das, A. J., Esquivel-Muelbert, A., Hammond, W. M., Martínez-Vilalta, J., McDowell, N. G., Powers, J. S., Pugh, T. A., Ruthrof, K. X., et al.: Climate change risks to global forest health: emergence of unexpected events of elevated tree mortality worldwide, Annual Review of Plant Biology, 73, 673–702, 2022.

Heinrich, V. H., Dalagnol, R., Cassol, H. L., Rosan, T. M., de Almeida, C. T., Silva Junior, C. H., Campanharo, W. A., House, J. I., Sitch, S., Hales, T. C., et al.: Large carbon sink potential of secondary forests in the Brazilian Amazon to mitigate climate change, Nature communications, 12, 1785, 2021.

Heinrich, V. H., Vancutsem, C., Dalagnol, R., Rosan, T. M., Fawcett, D., Silva-Junior, C. H., Cassol, H. L., Achard, F., Jucker, T., Silva, C. A., et al.: The carbon sink of secondary and degraded humid tropical forests, Nature, 615, 436–442, 2023.

Houghton, R., Hall, F., and Goetz, S. J.: Importance of biomass in the global carbon cycle, Journal of Geophysical Research: Biogeosciences, 114, 2009.

Houghton, R. A.: Revised estimates of the annual net flux of carbon to the atmosphere from changes in land use and land management 1850–2000, Tellus B: Chemical and Physical Meteorology, 55, 378–390, 2003.

Hu, T., Su, Y., Xue, B., Liu, J., Zhao, X., Fang, J., and Guo, Q.: Mapping global forest aboveground biomass with spaceborne LiDAR, optical imagery, and forest inventory data, Remote Sensing, 8, 565, 2016.

Huang, Y., Ciais, P., Santoro, M., Makowski, D., Chave, J., Schepaschenko, D., Abramoff, R. Z., Goll, D. S., Yang, H., Chen, Y., et al.: A global map of root biomass across the world's forests, Earth System Science Data, 13, 4263–4274, 2021.

Hubau, W., Lewis, S. L., Phillips, O. L., Affum-Baffoe, K., Beeckman, H., Cuní-Sanchez, A., Daniels, A. K., Ewango, C. E., Fauset, S., Mukinzi, J. M., et al.: Asynchronous carbon sink saturation in African and Amazonian tropical forests, Nature, 579, 80–87, 2020.

Kannenberg, S. A., Schwalm, C. R., and Anderegg, W. R.: Ghosts of the past: how drought legacy effects shape forest functioning and carbon cycling, Ecology letters, 23, 891–901, 2020.

https://doi.org/10.5194/essd-2026-246
Preprint. Discussion started: 12 May 2026

Konings, A. G., Rao, K., and Steele-Dunne, S. C.: Macro to micro: microwave remote sensing of plant water content for physiology and ecology, New Phytologist, 223, 1166–1172, 2019.

Kwon, M. J., Ballantyne, A., Ciais, P., Bastos, A., Chevallier, F., Liu, Z., Green, J. K., Qiu, C., and Kimball, J. S.: Siberian 2020 heatwave increased spring CO2 uptake but not annual CO2 uptake, Environmental Research Letters, 16, 124 030, 2021.

Lai, L., Huang, X., Yang, H., Chuai, X., Zhang, M., Zhong, T., Chen, Z., Chen, Y., Wang, X., and Thompson, J. R.: Carbon emissions from land-use change and management in China between 1990 and 2010, Science Advances, 2, e1601 063, 2016.

Lauerwald, R., Bastos, A., McGrath, M. J., Petrescu, A. M. R., Ritter, F., Andrew, R. M., Berchet, A., Broquet, G., Brunner, D., Chevallier, F., et al.: Carbon and greenhouse gas budgets of Europe: Trends, interannual and spatial variability, and their drivers, Global Biogeochemical Cycles, 38, e2024GB008 141, 2024.

Lewis, S. L., Brando, P. M., Phillips, O. L., Van Der Heijden, G. M., and Nepstad, D.: The 2010 amazon drought, Science, 331, 554–554, 2011.

Li, X., Ciais, P., Frappart, F., Scipal, K., Fan, L., Yang, H., Albergel, C., Liu, X., Liu, Y., Wang, M., et al.: IB-AGC: Annual 25 km global live biomass carbon product from SMOS L-band passive microwave vegetation optical depth, Scientific Data, 12, 1156, 2025.

Liu, G., Ciais, Philippe, T. S. Y. H., and Xiao, Chenwei, B. A.: A Moderate-Resolution, Long-Term Global Radar-Based Forest Above-Ground Biomass Dataset from 1993 to 2020, https://doi.org/10.5281/zenodo.19259660, 2026.

Liu, S., Bond-Lamberty, B., Hicke, J. A., Vargas, R., Zhao, S., Chen, J., Edburg, S. L., Hu, Y., Liu, J., McGuire, A. D., et al.: Simulating the impacts of disturbances on forest carbon cycling in North America: Processes, data, models, and challenges, Journal of Geophysical Research: Biogeosciences, 116, 2011a.

Liu, Y. Y., De Jeu, R. A., McCabe, M. F., Evans, J. P., and Van Dijk, A. I.: Global long-term passive microwave satellite-based retrievals of vegetation optical depth, Geophysical Research Letters, 38, 2011b.

Liu, Y. Y., Van Dijk, A. I., De Jeu, R. A., Canadell, J. G., McCabe, M. F., Evans, J. P., and Wang, G.: Recent reversal in loss of global terrestrial biomass, Nature Climate Change, 5, 470–474, 2015.

Mack, M. C., Walker, X. J., Johnstone, J. F., Alexander, H. D., Melvin, A. M., Jean, M., and Miller, S. N.: Carbon loss from boreal forest wildfires offset by increased dominance of deciduous trees, Science, 372, 280–283, 2021.

Manusch, C., Bugmann, H., Heiri, C., and Wolf, A.: Tree mortality in dynamic vegetation models–A key feature for accurately simulating forest properties, Ecological Modelling, 243, 101–111, 2012.

Matricardi, E. A. T., Skole, D. L., Costa, O. B., Pedlowski, M. A., Samek, J. H., and Miguel, E. P.: Long-term forest degradation surpasses deforestation in the Brazilian Amazon, Science, 369, 1378–1382, 2020.

McDowell, N. G., Coops, N. C., Beck, P. S., Chambers, J. Q., Gangodagamage, C., Hicke, J. A., Huang, C.-y., Kennedy, R., Krofcheck, D. J., Litvak, M., et al.: Global satellite monitoring of climate-induced vegetation disturbances, Trends in plant science, 20, 114–123, 2015.

Melton, J. R., Chan, E., Millard, K., Fortier, M., Winton, R. S., Martín-López, J. M., Cadillo-Quiroz, H., Kidd, D., and Verchot, L. V.: A map of global peatland extent created using machine learning (Peat-ML), Geoscientific Model Development, 15, 4709–4738, 2022.

Myneni, R. B., Dong, J., Tucker, C. J., Kaufmann, R. K., Kauppi, P. E., Liski, J., Zhou, L., Alexeyev, V., and Hughes, M.: A large carbon sink in the woody biomass of Northern forests, Proceedings of the National Academy of Sciences, 98, 14 784–14 789, 2001.

Pan, Y., Birdsey, R. A., Fang, J., Houghton, R., Kauppi, P. E., Kurz, W. A., Phillips, O. L., Shvidenko, A., Lewis, S. L., Canadell, J. G., et al.: A large and persistent carbon sink in the world's forests, science, 333, 988–993, 2011.

Pan, Y., Birdsey, R. A., Phillips, O. L., Houghton, R. A., Fang, J., Kauppi, P. E., Keith, H., Kurz, W. A., Ito, A., Lewis, S. L., et al.: The enduring world forest carbon sink, Nature, 631, 563–569, 2024.

https://doi.org/10.5194/essd-2026-246
Preprint. Discussion started: 12 May 2026

Phillips, O. L., Aragão, L. E., Lewis, S. L., Fisher, J. B., Lloyd, J., López-González, G., Malhi, Y., Monteagudo, A., Peacock, J., Quesada, C. A., et al.: Drought sensitivity of the Amazon rainforest, Science, 323, 1344–1347, 2009.

Piao, S., Friedlingstein, P., Ciais, P., Viovy, N., and Demarty, J.: Growing season extension and its impact on terrestrial carbon cycle in the Northern Hemisphere over the past 2 decades, Global Biogeochemical Cycles, 21, 2007.

Pickett, S. T.: Space-for-time substitution as an alternative to long-term studies, in: Long-term studies in ecology: approaches and alternatives, pp. 110–135, Springer, 1989.

Pongratz, J., Dolman, H., Don, A., Erb, K.-H., Fuchs, R., Herold, M., Jones, C., Kuemmerle, T., Luyssaert, S., Meyfroidt, P., et al.: Models meet data: Challenges and opportunities in implementing land management in Earth system models, Global change biology, 24, 1470–1487, 2018.

Pugh, T. A., Arneth, A., Kautz, M., Poulter, B., and Smith, B.: Important role of forest disturbances in the global biomass turnover and carbon sinks, Nature geoscience, 12, 730–735, 2019.

Qie, L., Lewis, S. L., Sullivan, M. J., Lopez-Gonzalez, G., Pickavance, G. C., Sunderland, T., Ashton, P., Hubau, W., Abu Salim, K., Aiba, S.-I., et al.: Long-term carbon sink in Borneo's forests halted by drought and vulnerable to edge effects, Nature communications, 8, 1966, 2017.

Qin, Y., Xiao, X., Wigneron, J.-P., Ciais, P., Brandt, M., Fan, L., Li, X., Crowell, S., Wu, X., Doughty, R., et al.: Carbon loss from forest degradation exceeds that from deforestation in the Brazilian Amazon, Nature Climate Change, 11, 442–448, 2021.

Reichstein, M., Bahn, M., Ciais, P., Frank, D., Mahecha, M. D., Seneviratne, S. I., Zscheischler, J., Beer, C., Buchmann, N., Frank, D. C., et al.: Climate extremes and the carbon cycle, Nature, 500, 287–295, 2013.

Saatchi, S. S., Harris, N. L., Brown, S., Lefsky, M., Mitchard, E. T., Salas, W., Zutta, B. R., Buermann, W., Lewis, S. L., Hagen, S., et al.: Benchmark map of forest carbon stocks in tropical regions across three continents, Proceedings of the national academy of sciences, 108, 9899–9904, 2011.

Santoro, M. and Cartus, O.: ESA Biomass Climate Change Initiative (Biomass_cci): Global datasets of forest above-ground biomass for the years 2010, 2017, 2018, 2019 and 2020, v4, (No Title), 2023.

Santoro, M. and Cartus, O.: ESA Biomass Climate Change Initiative (Biomass_cci): Global datasets of forest above-ground biomass for the years 2007, 2010, 2015, 2016, 2017, 2018, 2019, 2020, 2021 and 2022, v6.0, https://doi.org/10.5285/95913ffb6467447ca72c4e9d8cf30501, accessed: 2026-03-25, 2025.

Santoro, M., Cartus, O., Carvalhais, N., Rozendaal, D. M., Avitabile, V., Araza, A., De Bruin, S., Herold, M., Quegan, S., Rodríguez-Veiga, P., et al.: The global forest above-ground biomass pool for 2010 estimated from high-resolution satellite observations, Earth System Science Data, 13, 3927–3950, 2021.

Schepaschenko, D., Chave, J., Phillips, O. L., Lewis, S. L., Davies, S. J., Réjou-Méchain, M., Sist, P., Scipal, K., Perger, C., Herault, B., et al.: The Forest Observation System, building a global reference dataset for remote sensing of forest biomass, Scientific data, 6, 198, 2019.

Seidl, R., Fernandes, P. M., Fonseca, T. F., Gillet, F., Jönsson, A. M., Merganičová, K., Netherer, S., Arpaci, A., Bontemps, J.-D., Bugmann, H., et al.: Modelling natural disturbances in forest ecosystems: a review, Ecological modelling, 222, 903–924, 2011.

Shvetsov, E. G., Kukavskaya, E. A., Shestakova, T. A., Laflamme, J., and Rogers, B. M.: Increasing fire and logging disturbances in Siberian boreal forests: A case study of the Angara region, Environmental research letters, 16, 115 007, 2021.

Tagesson, T., Schurgers, G., Horion, S., Ciais, P., Tian, F., Brandt, M., Ahlström, A., Wigneron, J.-P., Ardö, J., Olin, S., et al.: Recent divergence in the contributions of tropical and boreal forests to the terrestrial carbon sink, Nature Ecology & Evolution, 4, 202–209, 2020.

https://doi.org/10.5194/essd-2026-246
Preprint. Discussion started: 12 May 2026

Tao, S., Ao, Z., Wigneron, J.-P., Saatchi, S., Ciais, P., Chave, J., Le Toan, T., Frison, P.-L., Hu, X., Chen, C., et al.: A global long-term, high-resolution satellite radar backscatter data record (1992–2022+): merging C-band ERS/ASCAT and Ku-band QSCAT, Earth System Science Data, 15, 1577–1596, 2023.

Tootchi, A., Jost, A., and Ducharne, A.: Multi-source global wetland maps combining surface water imagery and groundwater constraints, Earth System Science Data, 11, 189–220, 2019.

Tubiello, F. N., Conchedda, G., Wanner, N., Federici, S., Rossi, S., and Grassi, G.: Carbon emissions and removals from forests: new estimates, 1990–2020, Earth System Science Data, 13, 1681–1691, https://doi.org/10.5194/essd-13-1681-2021, 2021.

Tyukavina, A., Hansen, M. C., Potapov, P., Parker, D., Okpa, C., Stehman, S. V., Kommareddy, I., and Turubanova, S.: Congo Basin forest loss dominated by increasing smallholder clearing, Science advances, 4, eaat2993, 2018.

Uribe, M. d. R., Coe, M. T., Castanho, A. D., Macedo, M. N., Valle, D., and Brando, P. M.: Net loss of biomass predicted for tropical biomes in a changing climate, Nature Climate Change, 13, 274–281, 2023.

Vijay, V., Pimm, S. L., Jenkins, C. N., and Smith, S. J.: The impacts of oil palm on recent deforestation and biodiversity loss, PloS one, 11, e0159 668, 2016.

Walker, A. P., De Kauwe, M. G., Bastos, A., Belmecheri, S., Georgiou, K., Keeling, R. F., McMahon, S. M., Medlyn, B. E., Moore, D. J., Norby, R. J., et al.: Integrating the evidence for a terrestrial carbon sink caused by increasing atmospheric CO2, New phytologist, 229, 2413–2445, 2021.

Wang, J. A., Baccini, A., Farina, M., Randerson, J. T., and Friedl, M. A.: Disturbance suppresses the aboveground carbon sink in North American boreal forests, Nature Climate Change, 11, 435–441, 2021.

Wigneron, J.-P., Li, X., Frappart, F., Fan, L., Al-Yaari, A., De Lannoy, G., Liu, X., Wang, M., Le Masson, E., and Moisy, C.: SMOS-IC data record of soil moisture and L-VOD: Historical development, applications and perspectives, Remote Sensing of Environment, 254, 112 238, 2021.

Williams, C. A., Gu, H., MacLean, R., Masek, J. G., and Collatz, G. J.: Disturbance and the carbon balance of US forests: A quantitative review of impacts from harvests, fires, insects, and droughts, Global and Planetary Change, 143, 66–80, 2016.

Winkler, K., Yang, H., Ganzenmüller, R., Fuchs, R., Ceccherini, G., Duveiller, G., Grassi, G., Pongratz, J., Bastos, A., Shvidenko, A., et al.: Changes in land use and management led to a decline in Eastern Europe's terrestrial carbon sink, Communications Earth & Environment, 4, 237, 2023.

Xu, L., Saatchi, S. S., Yang, Y., Yu, Y., Pongratz, J., Bloom, A. A., Bowman, K., Worden, J., Liu, J., Yin, Y., et al.: Changes in global terrestrial live biomass over the 21st century, Science Advances, 7, eabe9829, 2021.

Xu, Y., Ciais, P., Santoro, M., Bourgoin, C., Ritter, F., Pellissier-Tanon, A., Feng, Y., Zhou, C., He, G., Heinrich, V., et al.: Small persistent humid forest clearings drive tropical forest biomass losses, Nature, 649, 375–380, 2026.

Yang, H., Ciais, P., Santoro, M., Huang, Y., Li, W., Wang, Y., Bastos, A., Goll, D., Arneth, A., Anthoni, P., et al.: Comparison of forest above-ground biomass from dynamic global vegetation models with spatially explicit remotely sensed observation-based estimates, Global Change Biology, 26, 3997–4012, 2020a.

Yang, H., Ciais, P., Frappart, F., Li, X., Brandt, M., Fensholt, R., Fan, L., Saatchi, S., Besnard, S., Deng, Z., et al.: Global increase in biomass carbon stock dominated by growth of northern young forests over past decade, Nature Geoscience, 16, 886–892, 2023.

Yang, L., Liang, S., and Zhang, Y.: A new method for generating a global forest aboveground biomass map from multiple high-level satellite products and ancillary information, IEEE Journal of Selected Topics in Applied Earth Observations and Remote Sensing, 13, 2587–2597, 2020b.

https://doi.org/10.5194/essd-2026-246
Preprint. Discussion started: 12 May 2026

Yang, Y., Saatchi, S. S., Xu, L., Yu, Y., Choi, S., Phillips, N., Kennedy, R., Keller, M., Knyazikhin, Y., and Myneni, R. B.: Post-drought decline of the Amazon carbon sink, Nature Communications, 9, 3172, 2018.

Yang, Y., Saatchi, S., Xu, L., Keller, M., Corsini, C. R., Aragão, L. E., Aguiar, A. P., Knyazikhin, Y., and Myneni, R. B.: Interannual variability of carbon uptake of secondary forests in the Brazilian Amazon (2004-2014), Global Biogeochemical Cycles, 34, e2019GB006 396, 2020c.

Yao, L., Liu, T., Qin, J., Jiang, H., Yang, L., Smith, P., Chen, X., Zhou, C., and Piao, S.: Carbon sequestration potential of tree planting in China, Nature Communications, 15, 8398, 2024.